Pis'ma v ZhETF, vol. 80, iss. 1, pp. 3 – 8

Induced photon emission from quark jets in ultrarelativistic heavy-ion collisions

B. G. Zakharov

L. D. Landau Institute for Theoretical Physics RAS, 117334 Moscow, Russia

Submitted 12 May 2004

We study the induced photon bremsstrahlung from a fast quark produced in AA-collisions due to multiple scattering in quark-gluon plasma. For RHIC and LHC conditions the induced photon spectrum is sharply peaked at photon energy close to the initial quark energy. In this region the contribution of the induced radiation to the photon fragmentation function exceeds the ordinary vacuum radiation. Contrary to previous analyses [4 – 7] our results show that at RHIC and LHC energies the final-state interaction effects in quark-gluon plasma do not suppress the direct photon production, and even may enhance it at $p_T \sim 5 - 15$ GeV.

PACS: 12.20.−m

1. In resent years much attention has been attracted to the direct photon production in AA-collisions at RHIC and LHC energies (see, for example, [1 – 3] and references therein). It is expected that for sufficiently small transverse momenta ($p_T \lesssim 3–4$ GeV) the dominating source of the direct photons at RHIC and LHC is radiation from quark-gluon plasma (QGP), and at higher p_T it is hard partonic mechanisms (Compton-process, quark-antiquark annihilation, and bremsstrahlung from fast quarks (antiquarks) produced in hard reactions) [1, 2]. Nuclear effects should modify the pQCD partonic contribution to the direct photons in AA-collisions as compared to that in pp interaction. For the Compton and annihilation processes which occur at small distances this modification, related to the initial state interaction (ISI) effects (nuclear shadowing and Cronin effect), is relatively small. However, one can expect strong final-state interaction (FSI) effects in the QGP for the bremsstrahlung which occurs at large distances. Investigation of the influence of the FSI on photon bremsstrahlung is of great interest from the point of view using the direct photons as a probe for the QGP at RHIC and LHC. It is especially important for LHC energies where the bremsstrahlung component is the dominating partonic mechanism [1, 4, 5].

It was suggested [4 – 7] that at RHIC and LHC the quark energy loss in the QGP phase due to the induced gluon radiation related to the multiple scattering should suppress strongly the bremsstrahlung contribution. At LHC energies it is equivalent to strong suppression of the total contribution of the pQCD mechanisms. In [4 – 7] it was assumed that the only effect of QGP on photon bremsstrahlung comes from the shift of the quark energy to a smaller value due to gluon emission before photon radiation. However, the analyses [4 – 7] missed two essential points. First of all, multiple scattering which fast quarks undergo in the QGP must enhance photon radiation due to the induced photon emission. Also, the assumption that all gluons are radiated before photon emission is not justified since the formation lengths for gluon and photon radiation are of the same order. In this case the gluons radiated after the photon do not suppress photon emission. For this reason one can expect that analyses [4 – 7] overestimate suppression of photon bremsstrahlung. In the present paper we address the photon bremsstrahlung at RHIC and LHC energies accounting for the induced photon radiation and the effect of finite gluon formation length.

2. The contribution of the bremsstrahlung mechanism to the cross section of photon production can be written as [8, 9]

$$\frac{d\sigma_{\gamma}^{AA}(p_T)}{dydp_T^2} = \int\limits_0^1 \frac{dx}{x^2} D_{q\to\gamma}(x, p_T/x) \frac{d\sigma_q^{AA}(p_T/x)}{dydp_T^2}, \quad (1)$$

where $d\sigma_q^{AA}(p_T)/dydp_T^2$ is the cross section of the processes $A + A \to q + X$ (hereafter we suppress the argument y and mean the central rapidity region $y \approx 0$), $D_{q\to\gamma}(x, E)$ is the fragmentation function for the $q \to \gamma q$ transition which accounts for all the FSI effects ($x = E_\gamma/E$, E_γ and E is the photon and initial quark energies, respectively). Summation over quark (antiquark) states is implicit on the right-hand side of (1). We write $D_{q\to\gamma}(x, E)$ in the form

$$D_{q\to\gamma}(x, E) = \frac{dP_{\mathrm{vac}}(x, E)}{dx} + \frac{dP_{\mathrm{ind}}(x, E)}{dx}. \quad (2)$$

The first term on the right-hand side of (2) is the probability distribution of the ordinary vacuum $q \to \gamma q$ splitting and the second one corresponds to the induced transition due to quark multiple scattering.

An accurate evaluation of the induced photon emission from a fast quark requires treatment of photon and multiple gluon radiation on an even footing. We begin with discussion of the induced $q \to \gamma q$ transition ignoring gluon radiation. A qualitative method for accounting for the gluon effects will be discussed later. To evaluate the induced spectrum we use the light-cone path integral approach [10] (see also [11–14]) which allows one to account for the Landau–Pomeranchuk–Migdal (LPM) effect [15, 16] and finite-size effects which play an important role in the problem of interest. The induced photon spectrum for a fast quark produced at $z=0$ can be written in a form similar to that for gluon emission given in [17] (we take z axis along the quark momentum)

$$\frac{dP_{\rm ind}}{dx} = \int\limits_0^\infty dz\, n(z) \frac{d\sigma_{\rm eff}^{BH}(x,z)}{dx}, \tag{3}$$

where $n(z)$ is the number density of the medium, and

$$\frac{d\sigma_{\rm eff}^{BH}(x,z)}{dx} = \mathrm{Re} \int d\boldsymbol{\rho}\, \Psi^*(\boldsymbol{\rho},x)\sigma(\rho x)\Psi_m(\boldsymbol{\rho},x,z) \tag{4}$$

is the in-medium (z-dependent) Bethe-Heitler cross section. Here $\sigma(\rho)$ is the dipole cross section of a quark-antiquark pair of size ρ with a particle in the medium. $\Psi(\boldsymbol{\rho},x)$ is the light-cone wave function for the $q\to\gamma q$ transition in vacuum, and $\Psi_m(\boldsymbol{\rho},x,z)$ is the in-medium light-cone wave function at the longitudinal coordinate z (we omit spin indices). The no spin flip wave functions, dominating the spectrum, read

$$\Psi(\boldsymbol{\rho},x) = P(x)\left(\frac{\partial}{\partial \rho_x{}'} - i s_g \frac{\partial}{\partial \rho_y{}'}\right) \times \\ \times \int\limits_0^\infty d\xi \exp\left(-\frac{i\xi}{L_f^\gamma}\right) \mathcal{K}_0(\boldsymbol{\rho},\xi|\boldsymbol{\rho}',0)\Big|_{\boldsymbol{\rho}'=0}, \tag{5}$$

$$\Psi_m(\boldsymbol{\rho},x,z) = P(x)\left(\frac{\partial}{\partial \rho_x{}'} - i s_g \frac{\partial}{\partial \rho_y{}'}\right) \times \\ \times \int\limits_0^z d\xi \exp\left(-\frac{i\xi}{L_f^\gamma}\right) \mathcal{K}(\boldsymbol{\rho},z|\boldsymbol{\rho}',z-\xi)\Big|_{\boldsymbol{\rho}'=0}, \tag{6}$$

where $P(x) = ie_q\sqrt{\alpha_{em}/2x}[s_\gamma(2-x)+2s_q x]/2M(x)$ ($s_{q,\gamma}$ denote quark and photon helicities), $L_f^\gamma = 2E(1-x)/m_q^2 x$ is the photon formation length, $\mathcal{K}$ is the Green's function for the two-dimensional Hamiltonian

$$\hat{H}(z) = -\frac{1}{2M(x)}\left(\frac{\partial}{\partial\boldsymbol{\rho}}\right)^2 - i\frac{n(z)\sigma(\rho x)}{2}, \tag{7}$$

with $M(x) = Ex(1-x)$, and

$$\mathcal{K}_0(\boldsymbol{\rho}_2,z_2|\boldsymbol{\rho}_1,z_1) = \frac{M(x)}{2\pi i(z_2-z_1)}\exp\left[\frac{iM(x)(\boldsymbol{\rho}_2-\boldsymbol{\rho}_1)^2}{2(z_2-z_1)}\right] \tag{8}$$

is the Green's function for the Hamiltonian (7) with $n(z)=0$.

The dipole cross section reads

$$\sigma(\rho) = C(\rho)\rho^2, \tag{9}$$

where

$$C(\rho) = \frac{C_T C_F}{\rho^2}\int d\mathbf{q}\,\alpha_s^2(q^2)\frac{[1-\exp(i\mathbf{q}\boldsymbol{\rho})]}{(q^2+\mu_D^2)^2}. \tag{10}$$

Here $C_{T,F}$ is the color Casimir for the medium constituents (quarks and gluons) and quark, μ_D is the Debye screening mass.

The effective Bethe-Heitler cross section (4) differs from that for a quark incident from infinity on an isolated scattering center due to the LPM effect and finite-size effects originating from the in-medium light-cone wave function entering (4). In the high-energy limit, when $L \ll L_f^\gamma$, here L is the thickness of the medium, the typical values of ρ become small ($\sim \sqrt{2L/Ex(1-x)}$), and the LPM effect can be neglected. In this case the spectrum is dominated by the $N=1$ scattering. In this regime the most important effect is modification of the in-medium light-cone wave function due to the finite-size effects. Let us first discuss the $N=1$ term to illustrate qualitatively the role of the finite-size effects. Neglecting the Q^2-dependence of α_s from (4)–(10) one can obtain

$$\frac{d\sigma_{\rm eff}^{BH}(x,z)}{dx} = \frac{\pi\alpha_{em}\alpha_s C_T C_F}{4E}\cdot\frac{(1-x+x^2/2)z}{(1-x)} \tag{11}$$

(hereafter for simplicity it is implied that $e_q=1$). The derivation of (11) is similar to that for gluon emission given in [18]. After substitution of (11) in (3) one obtains (for $n(z)$ =const) the spectrum $\propto L^2$

$$\frac{dP_{\rm ind}(x,E)}{dx} = \frac{\pi\alpha_{em}\alpha_s C_T C_F n L^2(1-x+x^2/2)}{8E(1-x)}. \tag{12}$$

One sees from (12) that in the high-energy limit contrary to the ordinary Bethe–Heitler spectrum $\propto 1/x$ the bremsstrahlung is $\propto 1/(1-x)$. Of course, formulas (11), (12) become invalid at $(1-x)\ll Lm_q^2/E$ when $L_f^\gamma \ll L$ and the spectrum reduces to the ordinary Bethe–Heitler one. It is worth noting that in the diagrammatic language the above formula for $N=1$ term corresponds to the set of diagrams shown in Fig.1. We would like to emphasize that the spectrum (12), similarly to the gluon

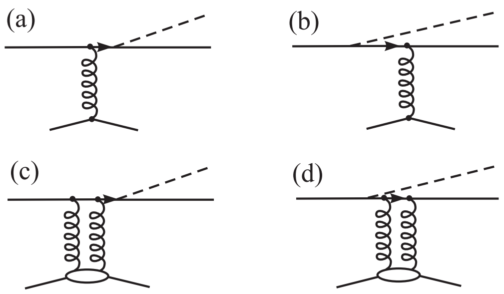

Fig.1. The set of Feynman diagrams corresponding to the $N=1$ scattering induced spectrum

spectrum of Ref. [18], cannot be obtained if one ignores the logarithmic ρ-dependence of the function $C(\rho)$ (10) at small ρ. One can see that, similarly to the gluon case, (11) and (12) do not contain any large logarithmic factor $\log(\mu_D\rho_{\rm eff})$ (here $\rho_{\rm eff}$ is the typical transverse scale) which one could expect there if one would neglect the ρ-dependence of $C(\rho)$.

The analytical formula (12) for the $N=1$ spectrum demonstrates that due to the finite-size effects at large energies, when $L_f^\gamma \gtrsim L$, the induced spectrum is strongly peaked at $x\approx 1$. As will be seen below the $N=1$ dominates for RHIC and LHC conditions, and the spectrum with the $N\geq 2$ scatterings included remains sharply peaked at x close to unity. Since the x-integral on the right-hand side of (1) is also dominated by large x one may expect that the induced photon emission to be an important source of the direct photons. It should be emphasized that our $1/(1-x)$ spectrum does not mean enhancement of radiation at large x. It originates simply from suppression of photon emission at small x due to the finite-size effects.

Now let us discuss the influence of the induced gluon emission on the photon bremsstrahlung ignored in the above derivation. The gluon emission, i.e., processes like $q\to\gamma g q$, and multi-gluon radiation, leads to quark energy loss, and should reduce radiation of hard photons. It is important that for soft gluons, dominating the quark energy loss, the gluon formation length, $L_f^g \sim \dfrac{2Ex(1-x)}{m_q^2x^2+m_g^2(1-x)}$, turns out to be of the same order as that for photons. For this reason, as was already noted, photon and gluon emission should be treated on an even footing. An accurate analysis with gluon emission is a complicated task which is far beyond the scope of the present paper. We account for influence of the induced gluon emission at qualitative level. In line with the prescription suggested in [19] for hadron spectra, we replace in (1) the cross section of quark production by an effective cross section

$$\frac{d\sigma^{AA}_{q,\rm eff}(p_T)}{dy\,dp_T^2} = N_{\rm bin}\int\frac{dx}{(1-x)^2}\times \times\frac{dI(x,p_T/(1-x))}{dx}\cdot\frac{d\sigma_q^{pp}(p_T/(1-x))}{dy\,dp_T^2}, \qquad (13)$$

where $dI(x,E)/dx$ is the probability distribution in the quark energy loss, and N_{bin} is the number of the binary nucleon-nucleon collisions. In the p_T-region of interest the cross section of quark production in pp collisions can be parametrized as [20]

$$\frac{d\sigma_q^{pp}(p_T)}{dy\,dp_T^2}\approx\frac{A}{(p_T+p_0)^n} \qquad (14)$$

with $p_0\approx 1.6\,$GeV, $n\approx 8$ for RHIC, and $p_0\approx 0.6\,$GeV, $n\approx 5.3$ for LHC, the normalization constant A will not be important to us. For such a p_T-dependence to good accuracy one can write the effective cross section of quark production as

$$\frac{d\sigma(p_T)^{AA}_{q,\rm eff}}{dy\,dp_T^2}\approx \approx N_{\rm bin}\frac{d\sigma_q^{pp}(p_T)}{dy\,dp_T^2}\cdot\int dx(1-x)^{n(p_T)-2}\cdot\frac{dI(x,p_T)}{dx}, \qquad (15)$$

where

$$n(p_T) = -\frac{d}{d\ln p_T}\ln\frac{d\sigma_q^{pp}(p_T)}{dy\,dp_T^2} = \frac{np_T}{(p_T+p_0)}.$$

Then the effective fragmentation function for photon radiation accounting for gluon emission can be written in the form

$$D^{\rm eff}_{q\to\gamma}(x,E) = S_g(E)\left[\frac{dP_{\rm vac}(x,E)}{dx}+\frac{dP_{\rm ind}(x,E)}{dx}\right], \qquad (16)$$

where $S_g(E)$ is the gluon suppression factor given by

$$S_g(E)\approx P_0(E)+\int\limits_{x_{\rm min}}^{1} dx(1-x)^{n(E)-2}\frac{dI(x,E)}{dx}.$$

Here we separated the probability of photon emission without gluons, P_0. In terms of the gluon spectrum, dP_g/dx, it reads

$$P_0(E) = \exp\left(-\int\limits_{x_{\rm min}}^{1} dx\frac{dP_g(x,E)}{dx}\right)$$

with $x_{\rm min}\sim m_g/E$. In numerical calculations we take $x_{\rm min}=2m_g/E$.

We take the spectrum in the radiated energy entering (13) in the form

$$\frac{dI(x,E)}{dx} = \exp\left(-\int_x^1 dy\frac{dP_g(y,E)}{dy}\right)\cdot\frac{dP_g(x,E)}{dx}. \qquad (17)$$

The formula (17) is similar to the electron energy loss spectrum derived in [21]. It works well for small energy loss $\Delta E \ll E$. For RHIC and LHC the parametrization (17) reproduces the energy loss spectrum evaluated assuming independent gluon radiation with accuracy $\sim 10-40\%$. It is enough to make qualitative estimate of the effect of gluon emission on the photon spectrum. An accurate calculation of the gluon suppression factor in the approximation of independent gluon emission [19, 22] does not make sense because this approximation itself does not have any serious theoretical justification. It should be noted that the suppression of hadron spectra evaluated using the energy loss spectrum (17) agrees well with that observed at RHIC. Thus, our approximation in some sense is justified by the experimental data.

Neglecting the ISI effects the nuclear modification factor defined as

$$R_{AA}(p_T) = \frac{1}{N_{\rm bin}}\cdot\frac{d\sigma_\gamma^{AA}(p_T)/dydp_T^2}{d\sigma_\gamma^{pp}(p_T)/dydp_T^2} \qquad (18)$$

can be approximately written as

$$R_{AA}(p_T) \approx S_g(p_T)\times$$
$$\frac{\int\limits_0^1 dx x^{n(p_T)-2}\left[dP_{\rm vac}(x,p_T)/dx + dP_{\rm ind}(x,p_T)/dx\right]}{\int\limits_0^1 dx x^{n(p_T)-2}dP_{\rm vac}(x,p_T)/dx}. \qquad (19)$$

We take the vacuum distribution in the form

$$\frac{dP_{\rm vac}(x,E)}{dx} = \frac{\alpha}{4\pi x}(4-4x+2x^2)\times$$
$$\times\int\limits_0^{k^2_{\rm max}} dk^2\frac{k^2}{(k^2+\epsilon^2)^2}, \qquad (20)$$

where $\epsilon = m_q x$, and $k_{\rm max} \approx E\max(x,(1-x))$.

To evaluate the gluon suppression factor S_g we use the formula for gluon spectrum similar to (3). However, we take the thickness equals $L/2$. It seems to be a reasonable choice to account for the fact that for $L_f^g \sim L_f^\gamma$ about half of gluons are radiated after photon emission and cannot affect the photon bremsstrahlung. Note that this reduces the suppression effect of gluon emission as compared with the analyses [4–7].

One remark is in order in connection with the above treatment of the gluon effects. Our gluon suppression factor includes only the induced gluon radiation. As far as the ordinary vacuum hard gluon radiation is concerned, we assume that, due to small formation length, the corresponding suppression factors are approximately the same for AA- and pp-collisions. For this reason one may ignore the vacuum gluon radiation in evaluating the nuclear modification factor (if one uses the leading order vacuum spectrum (20)).

3. For numerical calculations we use the one-loop running coupling constant with $\Lambda_{QCD} = 0.3$ GeV frozen at the value $\alpha_s = 0.7$. This parametrization is motivated by wanting to satisfy the relation

$$\int\limits_0^{2\,\rm GeV} dk\frac{\alpha_s(k)}{\pi} \approx 0.36 \text{ GeV} \qquad (21)$$

obtained from the analysis of the heavy quark energy loss [23]. To fix the quark and Debye screening mass we use the results of the analysis within the quasiparticle model [24] of the lattice results. For the relevant range of temperature of the plasma $T \sim (1-3)T_c$ ($T_c \approx 170$ MeV is the temperature of the deconfinement phase transition) the analysis [24] gives for the quark and gluon quasiparticle masses $m_q \approx 0.3$ and $m_g \approx 0.4$ GeV. With the above value of m_g from the perturbative relation $\mu_D = \sqrt{2}m_g$ one obtains $\mu_D \approx 0.57$ GeV. We assume the Bjorken [25] longitudinal expansion of the QGP with $T\tau^3 = T_0\tau_0^3$. For the initial conditions we use the values suggested in [20] $T_0 = 446$ MeV and $\tau_0 = 0.147$ fm for RHIC, and $T_0 = 897$ MeV and $\tau_0 = 0.073$ fm for LHC. For RHIC the above condition were obtained from the charged particle pseudorapidity density $dN/dy \approx 1260$ measured by the PHOBOS experiment [26] assuming an isentropic expansion and rapid thermolization at $\tau_0 \sim 1/3T_0$. The LHC parameters correspond to $dN/dy \approx 5625$ estimated in [27]. Note that, since the dominating ρ-scale in (3) $\propto \sqrt{z}$ for $z \ll L_f^\gamma$, our results are not very sensitive to τ_0. For the upper limit of the z-integration in (21) we take[1)]. $L = R_A \approx 6$ fm This seems to be a reasonable value for central heavy-ion collisions since due to the transverse expansion the hot QCD matter should cool quickly at $\tau \gtrsim R_A$ [25].

In Figs.2 and 3 we show the x-dependence of the probability distribution of the induced $q \to \gamma q$ transition (solid line) for several quark energies for RHIC

[1)] For our choice of the initial conditions the life-time of QGP is ~ 3 fm for RHIC. However, in the interval $\tau \sim 3-6$ fm the density of the mixed phase is practically the same as that for the pure QGP phase.

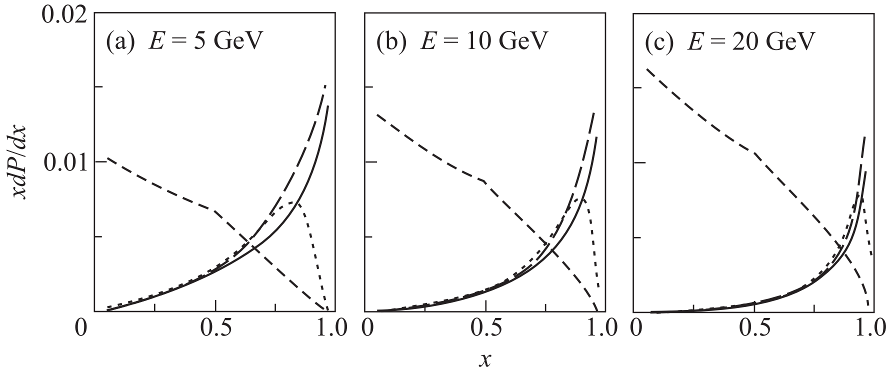

Fig.2. The photon spectrum of the $q \to \gamma q$ transition for RHIC conditions. The solid line shows contribution from the induced photon emission calculated using the formula (3). The dashed line shows the vacuum spectrum (20). The $N = 1$ scattering contribution to the induced spectrum is shown by the long-dashed curves for infinite kinematic boundaries, and by the dotted curves for finite kinematic boundaries

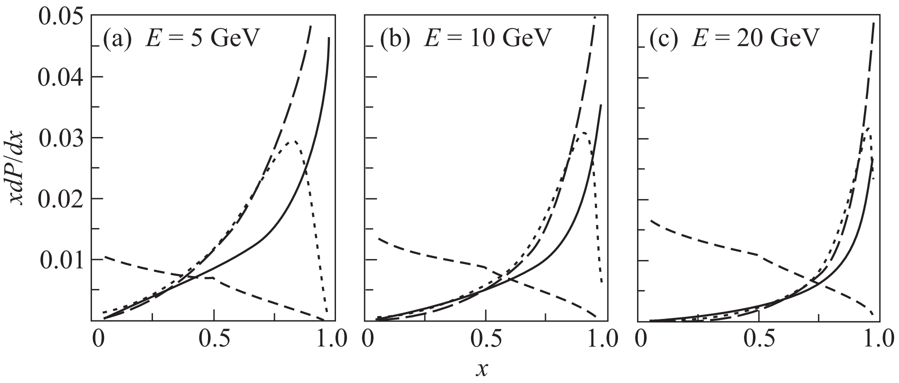

Fig.3. The same as in Fig.2 but for LHC

and LHC. For comparison the vacuum spectrum (dashed line) is also shown. One sees that in the region of large x, which dominates the x-integrals on the right-hand side of Eq. (19), the induced radiation exceeds the vacuum one (especially for the LHC case). To illustrate the influence of the LPM effect on the induced photon emission we also show the contribution of the $N = 1$ scattering (long-dashed line). It is seen that for $x \sim 0.6 - 0.8$ the LPM effect reduces the induced bremsstrahlung by a factor of ~ 0.8 for RHIC and ~ 0.5 for LHC. Note that the LPM effect and finite-size effects diminish in strength as $x \to 1$ since L_f^γ becomes small and the spectrum should be close the Bethe-Heitler one in this limit. To demonstrate the role of the finite kinematic limits (neglected in (3)) in Figs.2, 3 we also show the $N = 1$ scattering contribution evaluated using the set of diagrams shown in Fig.1 with finite kinematic limits (dotted line). One can see that the kinematic effects become important at x close to unity. Numerical calculations show that they reduce the integral over x in the numerator in (19) by $\sim 20-30\%$. However, this suppression to good accuracy is compensated by the increase in the gluon suppression factor due to similar kinematic effects for gluon emission. For this reason we neglect the kinematic effects in calculation of the nuclear modification factor (19).

In Fig.4 we plot results for the p_T-dependence of the nuclear modification factor (19). We also show the results without gluon suppression factor (dashed line),

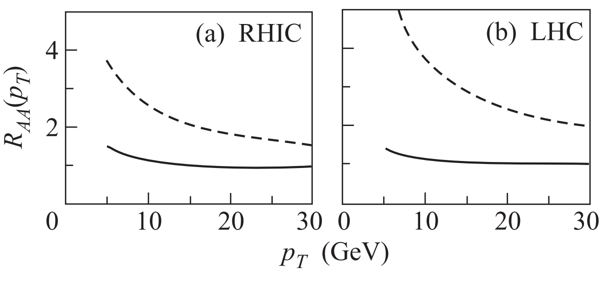

Fig.4. The p_T-dependence of the nuclear modification factor (19) (solid line) for RHIC (a) and LHC (b) conditions. The dashed line shows the results without gluon suppression factor S_g on the right-hand side of (19)

i.e., for $S_g = 1$. One sees that despite strong suppression due to gluon emission we obtain $R_{AA} \gtrsim 1$ at

$p_T \sim 5-15\,\mathrm{GeV}$. This means that the FSI effects can enhance the direct photon production (especially for LHC energies, where bremsstrahlung is the dominating partonic mechanism). Of course, one should bear in mind that uncertainties in our theoretical predictions can be about $30\div50\%$. Nevertheless, one can say that it is practically excluded that in central AA-collisions the direct photon production is strongly suppressed due to quark energy loss, as was predicted in [4 − 7].

I am grateful to S. Peigne for discussions. I thank especially P. Aurenche for discussions and useful comments on the paper. I am also grateful to the LAPTH and the High Energy Group of the ICTP for the kind hospitality during my visits to Annecy and Trieste where a part of this work was done.

1. P. Aurenche, *LAPTH-CONF-893-2001, Jan 2002, Talk given at International Workshop on the Physics of the Quark Gluon Plasma*, Palaiseau, France, 4–7 Sep 2001, hep-ph/0201011.
2. T. Peitzmann and M. H. Thoma, Phys. Rept. **364**, 175 (2002).
3. F. Arleo, P. Aurenche, F. Bopp et al., *The CERN Yellow Report on Hard Probes in Heavy Ion Collisions at the LHC*, hep-ph/0311131.
4. A. Dumitru and N. Hammon, hep-ph/9807260 (1998).
5. J. Jalilian-Marian, K. Orginos, and I. Sarcevic, Nucl. Phys. **700**, 523 (2002).
6. J. Jalilian-Marian, K. Orginos, and I. Sarcevic, Phys. Rev. **C63**, 041901 (2001).
7. S. Jeon, J. Jalilian-Marian, and I. Sarcevic, Phys. Lett. **B562**, 45 (2003).
8. J. F. Owens, Rev. Mod. Phys. **59**, 465 (1987).
9. P. Aurenche, R. Baier, M. Fontannaz, and D. Schiff, Nucl. Phys. **B297**, 661 (1988).
10. B. G. Zakharov, JETP Lett. **63**, 952 (1996).
11. B. G. Zakharov, JETP Lett. **65**, 615 (1997).
12. B. G. Zakharov, Phys. Atom. Nucl. **61**, 838 (1998).
13. B. G. Zakharov, JETP Lett. **70**, 176 (1999).
14. R. Baier, D. Schiff, and B. G. Zakharov, Ann. Rev. Nucl. Part. **50**, 37 (2000).
15. L. D. Landau and I. Ya. Pomeranchuk, Dokl. Akad. Nauk SSSR **92**, 535, 735 (1953).
16. A. B. Migdal, Phys. Rev. **103**, 1811 (1956).
17. B. G. Zakharov, *Proc. of the at 33rd Rencontres de Moriond: QCD and High Energy Hadronic Interactions*, Ed. J. Tran Thanh Van, Les Arcs, France, 21–28 Mar 1998, p. 533; hep-ph/9807396.
18. B. G. Zakharov, JETP Lett. **73**, 49 (2001).
19. R. Baier, Yu. L. Dokshitzer, A. H. Mueller, and D. Schiff, JHEP **0109**, 033 (2001); hep-ph/0106347 (2001).
20. R. J. Fries, B. Müller, and D. K. Srivastava, nucl-th/0208001 (2003).
21. B. G. Zakharov, Phys. Atom. Nucl. **62**, 1008 (1999); JETP Lett. **78**, 759 (2003).
22. M. Gyulassy, P. Levai, and I. Vitev, Phys. Lett. **B538**, 282 (2002).
23. Yu. L. Dokshitzer, V. A. Khoze, and S. I. Troyan, Phys. Rev. **D53**, 89 (1996).
24. P. Levai and U. Heinz, Phys. Rev. **C57**, 1879 (1998).
25. J. D. Bjorken, Phys. Rev. **D27**, 140 (1983).
26. B. B. Back et al. [PHOBOS Collaboration], Phys. Rev. **C65**, 061901 (2002).
27. J. Kapusta, L. D. McLerran, and D. K. Srivastava, Phys. Lett. **B283**, 145 (1992).